Journal of Microelectronics and Electronic Packaging (2023) **20**, 9–16
Copyright © International Microelectronics Assembly and Packaging Society
ISSN: 1551-4897

Electromigration Risk Assessment and Circuit Optimization Using Innovative Multiphysics Modeling

Chongyang Cai,[1] Zhi Yang,[1,*] Yuan Li,[1] Padam Jain,[1] Terry Kang,[1] and Krishna Mellachervu[2]

***Abstract*—With smaller and denser transistors, the physical flow of electrons may inhibit the performance of the device over time by forming voids and cracks at interconnects due to electromigration (EM). Circuit designs that fail to meet EM specifications may lead to catastrophic failures and SI/PI performance degradation. One way of mitigating EM is to use multiple vias between layers of copper traces to reduce the current crowding effect. However, the quantities of vias may affect the current density and current redistribution inside critical joints. Current studies mainly focus on predicting the EM time-to-failure (TTF) based on the empirical Black's equation. However, this method may not give enough insights about void formation and crack propagation, and reflects the current redistribution that could impact the TTF. In this study, we compared the EM lifetime of ball grid array (BGA) test vehicles with different structural designs and developed a methodology to consider the diffusion of atoms in solder joints based on Multiphysics field migration to study the current redistribution influence of vias. Moreover, crack propagation was also simulated to understand the failure mechanism. BGA traces without vias and with 8 vias are stressed under 5A, 7A, and 9A at 150°C to compare the EM performance. Moreover, each test structure is manufactured with two different surface finishes: A and B. Based on the experimental results, finite element analysis (FEA) simulations based on Atom Flux Divergence (AFD) were performed to compare with the experiment results. It was found that the current crowding effect could be significantly reduced by 8 vias compared with daisy-chained traces. The study shows better EM resistance with 8 and 4 vias than no-via traces and helps predict the EM life of different structures to provide guidance for design optimization.**

***Keywords*—Electromigration, reliability, Multiphysics, finite element analysis, circuit optimization**

Introduction

With the development and minimization trend of electronic components and products, microelectronic interconnections have been designed with continuously decreasing scale and pitch [1]. With each silicon node, current delivery to the conductors is becoming increasingly higher and generates elevated temperatures due to joule heating [2]. Electromigration (EM) is one of the most critical failures that need to be considered for structures under higher current input. The physical flow of electrons will inhibit the performance of devices and lead to voids and open circuitry due to the electron momentum transferred to atoms as shown in Fig. 1 [3].

Many studies have been done to evaluate the EM risk and the most commonly used empirical equation to assess the time-to-failure (TTF) is Black's equation.

$$MTTF = \frac{A}{j^n}\exp\left(\frac{E_a}{k_b T}\right) \tag{1}$$

where, j is the current density, T is the local temperature, A is a constant, E_a is activation energy, and K_b is Boltzmann's constant [4]. The EM resistance is related to the thermal-electric input. However, EM in real life is a Multiphysics diffusion phenomenon that couples thermal electrical as well as stress migration [5]. Moreover, the empirical equation may not be capable of characterizing the current crowding effects and thus, has limits in providing more insights into the failure mechanism.

To model the current distribution and the diffusion process in interconnects, some research has been done to simulate the process. Atom Flux Divergence (AFD) theory is proposed based on the Fick's law to describe the atomic flux behavior under different physics fields [6]. Some studies performed simulations to characterize the current distribution and the divergence of atoms [7, 8], yet the static analysis may lack experimental verification and could not simulate the crack propagation procedure to cause open circuitry. In this study, a finite element analysis (FEA) based on AFD is performed to investigate the transient void initiation and crack propagation process. Two different structures: ball grid array (BGA) trace without vias and BGA with 8 vias are tested under the condition of 5A, 7A, and 9A at 150°C to study the influence of vias in current redistribution and improving EM life. The vias for

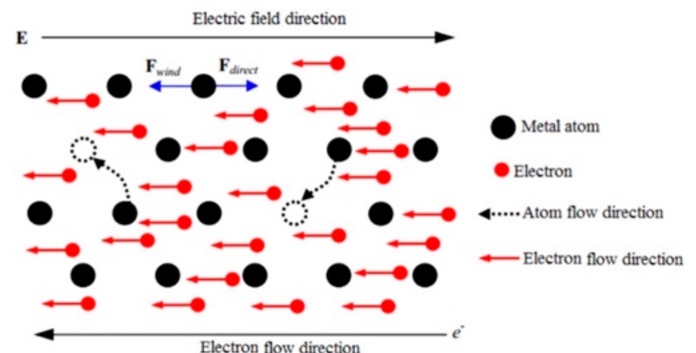

Fig. 1. Schematic of atoms moving under electron wind.

The manuscript was received on January 3, 2023; revision received on February 7, 2023; accepted on February 9, 2023.
The original version of this article was presented at the 55th International Symposium on Microelectronics (IMAPS'2022) in Boston, MA, USA, October 3-6, 2022.
[1]Google Inc., Sunnyvale, California
[2]ANSYS Inc., San Jose, California
*Corresponding author; email: yzhi@google.com

doi:10.4071/imaps.1882247
1551-4897 © 2023 International Microelectronics Assembly and Packaging Society

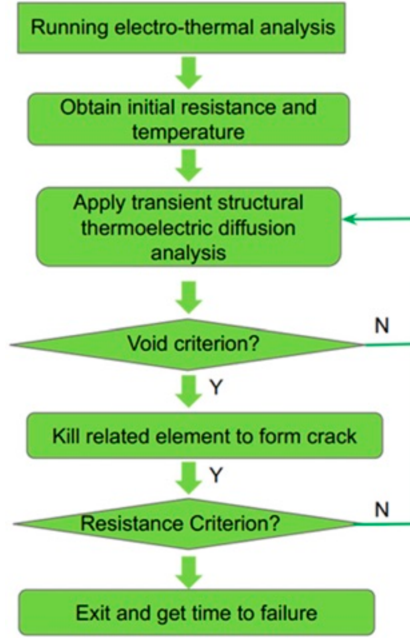

Fig. 2. Flow chart of performing Multiphysics modeling.

the test vehicles are drilled holes. Besides, the test vehicles are manufactured with two different surface finishes A and B. In this article, to simulate the diffusion barrier effects of surface finish, the void concentration is used as the threshold. The modeling methodology can correct the experimental testing data and help provide an estimation of EM life with different trace designs so that it can provide guidelines for circuit design optimization.

Methodology

In reality, the atoms are driven under the electron winds during the EM process, where near the upwind side voids will form and downwind side hillocks will accumulate. The phenomenon involves different physics fields including electron wind migration, temperature gradient migration, and stress gradient migration. According to AFD theory, the coupling diffusion flux is the superposition of atom flux under different physics fields. The different migration fluxes under different driven forces are listed [9-11].

A. Electron Wind Migration

The atoms moving under the electric field will collide with electrons and cause drastic momentum exchange. The driving force can be obtained as shown:

$$\overrightarrow{F_{ew}} = \overrightarrow{F_{direct}} + \overrightarrow{F_{wind}} = Z^* e\rho j \tag{2}$$

Table II
Material Properties for EM

Material properties	Cu	SAC305
	Structural	
Modulus (MPa)	127e3	26.2e3
CTE (ppm/C)	17.1	23
v	.31	.35
Atomic volume Ω (m^3)	1.182e−29	2.71e−29
	Thermal	
Conductivity k (W/m·K)	393	57
Specific heat (J/kg·K)	385.2	219
Density (kg/m^3)	8900	7390
Heat of transport (eV)	.3121	.0094
	Electric	
Resistivity ρ (Ω·m)	2.52e−8	18.1e−8
Effective charge number Z^*	−4	−23
	Diffusion	
Diffusivity D_0 (m^2/s)	7.8e−5	4.1e−8
Activation energy E_a (eV)	1.2	.8

where, $\overrightarrow{F_{direct}}$ is the Coulomb force and $\overrightarrow{F_{wind}}$ is the electron wind, $\overrightarrow{F_{ew}}$ is the total force. Z^* is the effective charge number, ρ is the resistivity, and j is the local current density. The electron wind caused migration flux can be described as:

$$\overrightarrow{J_{ew}} = \frac{c}{k_b T} D_0 \exp\left(-\frac{E_a}{k_b T}\right) e Z^* j\rho \tag{3}$$

$$div(\overrightarrow{J_{ew}}) = \left(\frac{Ea}{k_b T} - \frac{1}{T} + \alpha\frac{\rho_0}{\rho}\right)\overrightarrow{J_{ew}} \nabla T + \frac{1}{C}\overrightarrow{J_{ew}} \nabla C \tag{4}$$

$$\rho = \rho_0[1 + \alpha(T - T_0)] \tag{5}$$

where, α is the temperature coefficient of resistivity, ρ_0 is the resistivity at T_0, C is the atomic concentration where atomic volume $\Omega = 1/C$, the atomic volume is a very small value, thus, the second term of $div(\overrightarrow{J_{ew}})$, $\frac{1}{C}\overrightarrow{J_{ew}}\nabla C$, can be simplified.

B. Thermal Migration

Joule heating will be generated when the current passes through the conductors. The different heat dissipation at different structure locations will introduce temperature variance. Such a temperature gradient will drive atoms to move from areas that have a higher temperature to areas that have a lower temperature. The driving force of thermal migration can be derived as:

$$\overrightarrow{F_{th}} = Q^* \frac{\nabla T}{T} \tag{6}$$

where, force is related to the gradient of temperature and Q^* is the heat of transport. The thermal migration flux can be

Table I
Comparison of Different Approaches

	Empirical Black's equation	Proposed FEM approach
Physics field	Thermal-electric	Multiphysics (thermal-electric stress diffusion)
Failure criterion	Tuned for fixed condition	Flexible for different resistance criterion
Failure mechanism simulation	No	Simulate void initiation and crack propagation
Design rule spec setup	Limited	More insights

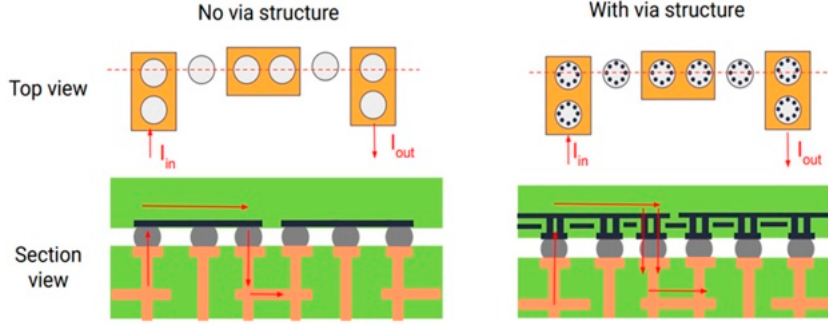

Fig. 3. Schematic of two different test vehicle designs.

described as:

$$\overrightarrow{J_{th}} = \frac{c}{k_b T} D_0 \exp\left(-\frac{E_a}{k_b T}\right) Q^* \frac{\nabla T}{T} \tag{7}$$

And the flux divergence can be calculated as shown as follows:

$$div(\overrightarrow{J_{th}}) = \left(\frac{Ea}{k_b T} - \frac{3}{T} + \alpha\frac{\rho_0}{\rho}\right)\overrightarrow{J_{th}}\nabla T + \frac{CQ^* D}{3k_b^3 T^3} j^2 \rho^2 e^2 + \frac{1}{C}\overrightarrow{J_{th}}\nabla C \tag{8}$$

The last term $\frac{1}{C}\overrightarrow{J_{th}}\nabla C$ can be similarly simplified.

C. Stress Migration

Stress gradient-induced migration (SM) was first introduced by Blech, which is called back stress. The CTE mismatch of the interconnect materials will generate thermal stress when the local temperature is different from the stress-free temperature. This stress will push the atom to move along the stress gradient [12, 13].

The driving force of stress gradient can be written as:

$$\overrightarrow{F_{ew}} = \Omega \nabla \sigma_H \tag{9}$$

where, σ_H is the hydrostatic stress. The stress migration flux can be shown as follows:

$$\overrightarrow{J_s} = \frac{c}{k_b T} D_0 \exp\left(-\frac{E_a}{k_b T}\right) \Omega \nabla \sigma_H \tag{10}$$

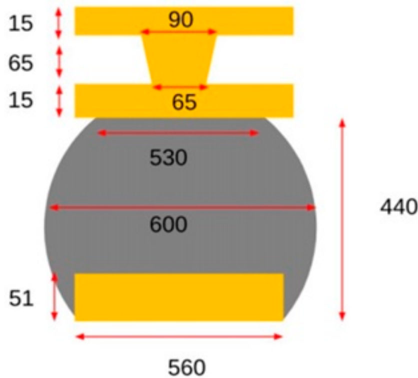

Fig. 4. Dimension of solder joint with vias (μm).

The flux divergence can be described as:

$$div(\overrightarrow{J_s}) = \left(\frac{Ea}{k_b T} - \frac{1}{T}\right)\overrightarrow{J_s}\nabla T + \frac{C\Omega D}{k_b T} div(\nabla \sigma_H) \tag{11}$$

In summary, the governing equation to model the Multiphysics diffusion can be summarized as:

$$\overrightarrow{J_{total}} = \frac{c}{k_b T} D_0 \exp\left(-\frac{E_a}{k_b T}\right)\left(eZ^* j\rho + Q^* \frac{\nabla T}{T} + \Omega \nabla \sigma_H\right) \tag{12}$$

Based on the governing equation describing the atom behavior during EM, the vacancy/atom concentration of elements can be obtained by modeling. The flow chart of conducting the Multiphysics modeling is shown in Fig. 2. In the first step, only electrothermal analysis is performed. The objective of the static analysis is to obtain the initial temperature distribution and apply it as the input for transient analysis. Based on the available temperature, the Multiphysics modeling is performed where the element vacancy concentration is used as a criterion to execute void initiation in the loop. Once the vacancy concentration of a certain element reaches the threshold, we consider that the element has evolved into a void, so the element is killed and the geometry of the model will be updated. Meanwhile, the voltage of the conductive parts, which represents the resistance increase of the structure, is also examined. Once the structure reaches a 15% resistance increase, the simulation will stop and be considered a failure of the entire structure.

The abovementioned process brings another advantage to the modeling methodology. Compared with empirical Black's equation estimation that has a fixed resistance increase criterion, the criterion of resistance increase can be adjusted flexibly according to the actual experimental criterion.

The summarized comparison of Multiphysics modeling and empirical Black's equation is shown in Table I.

The material parameters input for the equation are listed in Table II [9, 14].

The test vehicle structures under current stressing are shown in Fig. 3. Two types of packages are compared—one structure has copper traces daisy-chained on the PCB side without vias and the other structure has 8 vias located at the peripheral area of the pad. The dark lines are copper traces in the substrate. Both structures are polarized and all current stressing is concentrated on the central two victim solder joints. Each structure has two different surface finishes: A and B. The structures are

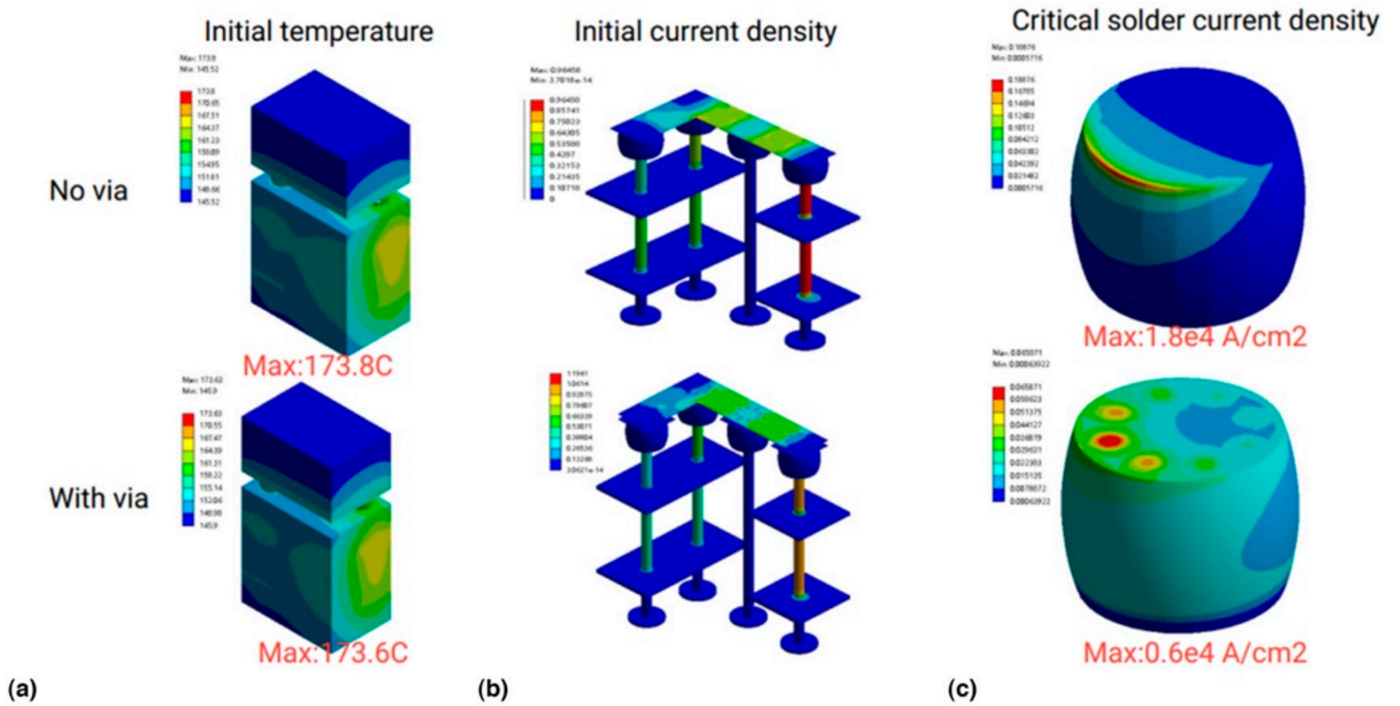

Fig. 5. Time zero temperature and current density distribution at 150°C and 5A: (a) temperature, (b) current density in conductors, and (c) current density in victim solder.

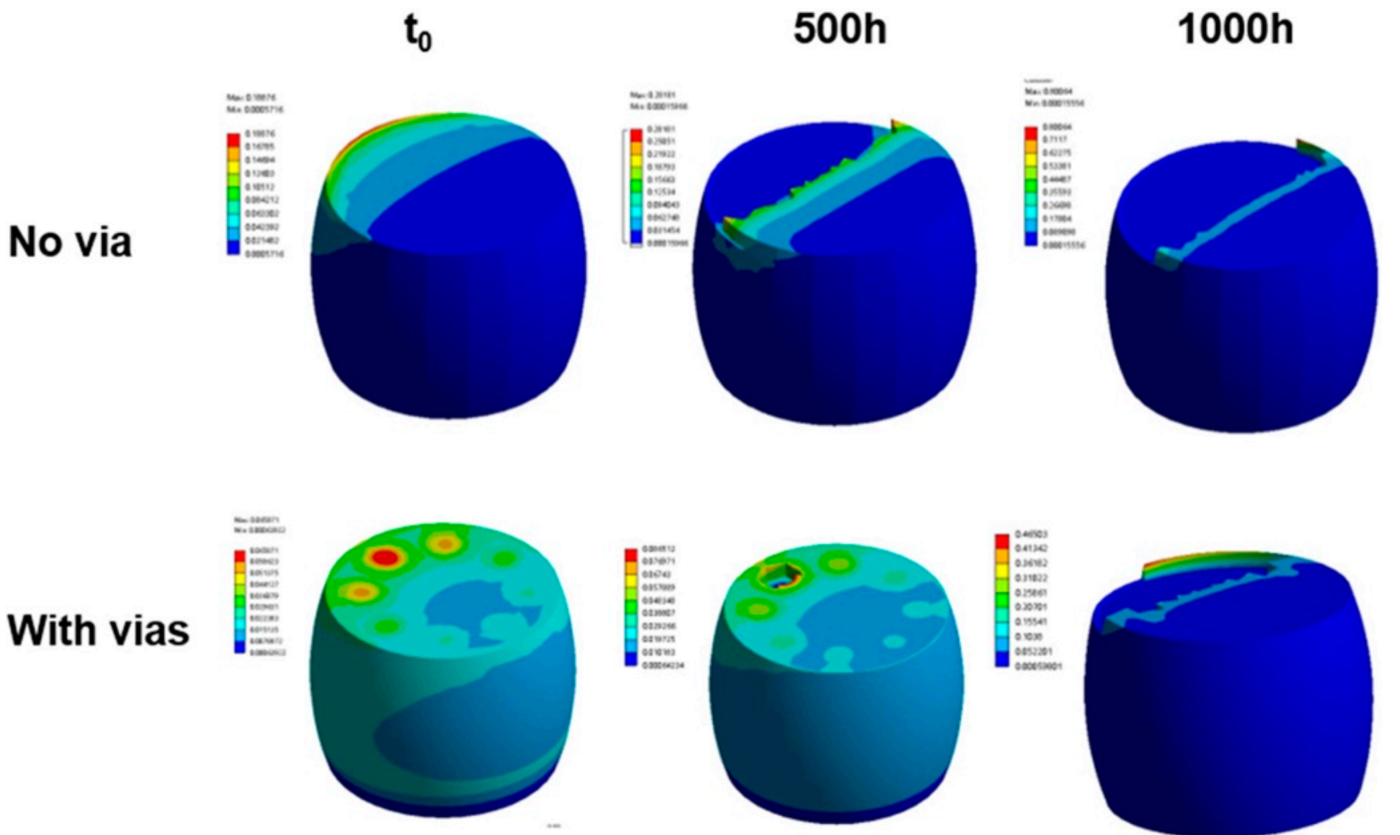

Fig. 6. Void evolution and current density change during EM.

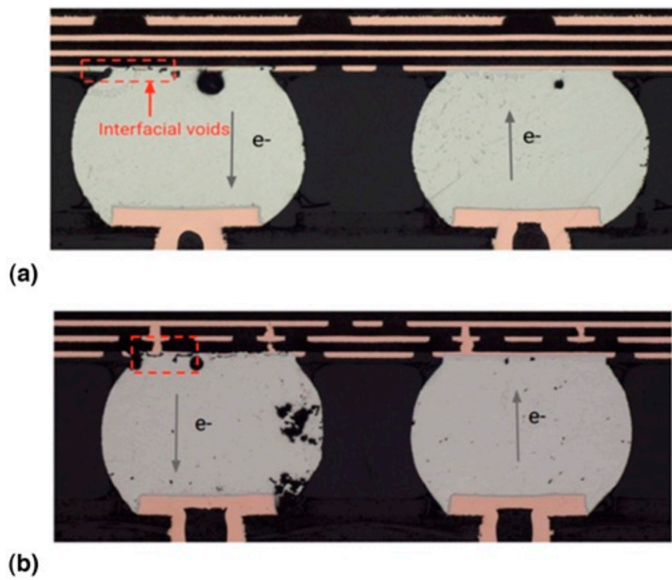

Fig. 7. Void evolution and current density change during EM: (a) structure without vias and (b) structure with 8 vias.

placed under the current stressing of 5A, 7A, and 9A at 150°C. When the resistance peak has an increase of 15%, the structures will be considered failures. The solder joint with vias is shown in Fig. 4, the taper via has an upper diameter of 90 µm and a bottom diameter of 65 µm.

The simulation is correlated and validated by experimental test results.

Results and Discussion

After static thermal-electric analysis, the initial temperature and current distribution can be obtained. The film coefficient is correlated as 1,000 W/m^2·C for the half symmetric model. As shown in Fig. 5a, when both structures are under the 5A and 150°C conditions, the joule heating effect of no-via structures and structures with vias is compared. In previous studies, it is found that using single via design may cause significant joule heating and result in earlier failure of the structure. However, in this study, although both structures show temperature increase compared with ambient temperature, the structure without vias has a similar highest temperature to the structure that has 8 vias. The multiple vias help share the current loading so that each via has a lower current density. It can be validated in Fig. 5c that the maximum current density of the victim solder of structure without vias is 1.8e4 A/cm^2. Due to the current crowding effect, the highest current density is located at the entrance location of the current. However, for the structure with 8 vias, the maximum current density is much smaller, around .6e4 A/cm^2. The current crowding effect still exists in the via structure, the current density is the highest underneath the via near the current entrance location, and such via can be considered as a critical via. The current density reduces in other vias that are far from the critical via.

The temperature can be applied to the transient Multiphysics analysis, with the diffusion proceeds, the element vacancy concentration will increase and generate cracks. As shown in Fig. 6, voids will form and further propagate due to the increase in vacancy concentration. Meanwhile, the crack will intensify the current crowding and cause a further increase in maximum current density, which leads to final failure. The void initiates near the location that has maximum current density, for a structure without vias, it forms at the soldered edge and propagates toward the other side. However, for a structure that has 8 vias, the void appears underneath the critical via and expands gradually in other directions.

The variance of the failure mechanism in modeling can be verified. In Fig. 7a, the test vehicle without vias has the interfacial voids initiated at the edge and in Fig. 7b, the cracks expand along both directions around the critical via in the test vehicle with 8 vias. In both structures, voids generate at the upwind side of the electron wind. Moreover, the resistance increase in modeling is compared with the experimental data, which shows a similar increase in resistance when the crack propagates along the interface as shown in Fig. 8.

In order to correlate the modeling TTF to actual experiment results, the vacancy concentration threshold needs to be tuned. Moreover, it can be used as the parameter to characterize the

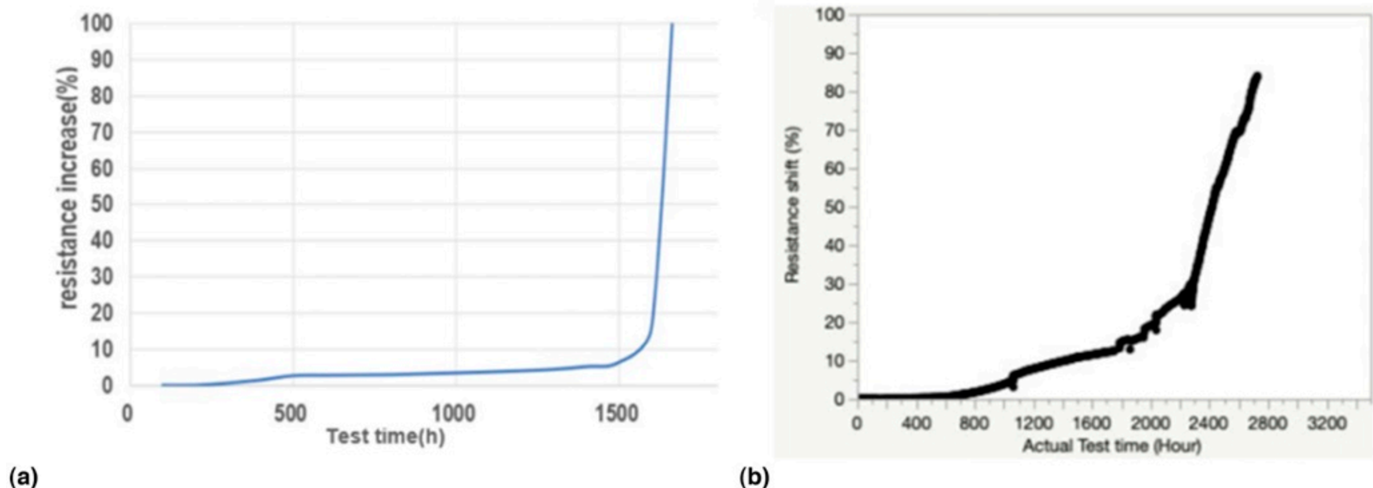

Fig. 8. Void evolution and current density change during EM: (a) simulation resistance increase and (b) experiment resistance increase.

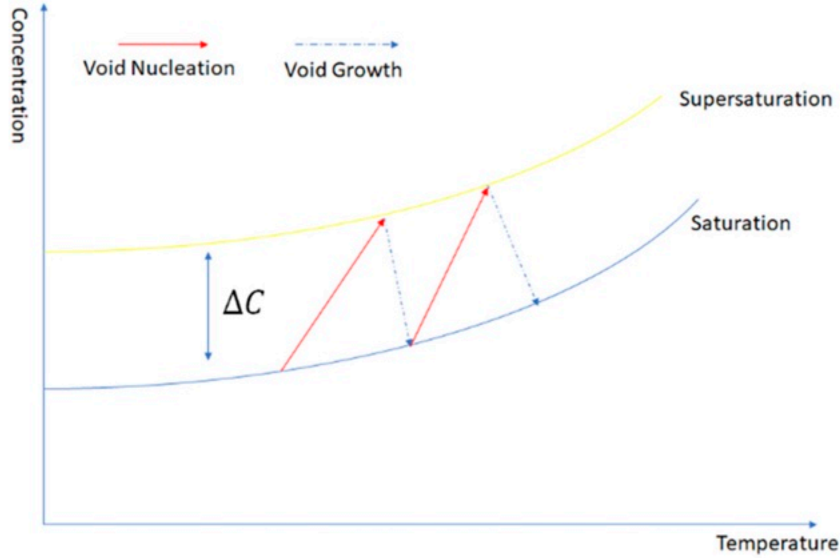

Fig. 9. Failure criteria adjustment based on temperature.

diffusion barrier effect [15] when the test structure has different surface finishes. In the modeling, we describe the critical concentration as:

$$C_{critical} = A \cdot f(j) \cdot f(T) \tag{13}$$

where, A is a constant, $f(j)$ is a function related to the feeding current since the IMC growth is related to the current value [16], the $A \cdot f(j)$ can be expressed as $A \cdot j^n$—where n is the current exponent and this term can be used to characterize the diffusion influence introduced by the surface finish. $f(T)$ is a function related to temperature, as shown in Fig. 9, the failure criterion is adjusted during the modeling because when the void is generated, the local temperature will increase thus, the adjustment of $f(T)$ can be written in the form of updated critical concentration [17]:

$$f(T) = C_{initial} \cdot \exp\left(-\frac{1}{k_b T_{new}}\right) / \exp\left(-\frac{1}{k_b T_{initial}}\right) \tag{14}$$

where, the T_{new} is the increased temperature, $C_{initial}$ and $T_{initital}$ are the initial vacancy concentration and initial local temperature.

Table III
Experiment and Modeling TTF of Two Surface Finishes in Structures Without Vias

Current (A)	Experiment TTF (h)	Modeling TTF (h)	Error
Surface finish A			
5	1,483	1,400	12%
7	214	*200*	*6%*
9	83	100	20%
Surface finish B			
5	5,148	4,900	4%
7	683	*700*	*2.4%*
9	433	500	15.4%

As a result, we are able to correlate the critical vacancy concentration threshold parameters to the experimental testing TTF data. As shown in Table III, by correlating the experimental data of structures without vias under 5A and 9A. The structure with vias shows no failure till 2000 h, so the parameters are fitted with the structure without vias. The constant A and n can be fitted for A and B surface finish. For A, $C_{critical}$ can be expressed as:

$$C_{critical} = 5.5 \cdot j^{-0.74} \cdot f(T) \tag{15}$$

The critical concentration for B can be fitted as:

$$C_{critical} = 2.39 \cdot j^{-0.14} \cdot f(T) \tag{16}$$

With the available fitted parameters, it is possible to predict the modeling TTF of structures under 7A, as shown in Table III, the underlined results are compared to show the consistency with the experimental data, which proves the validity of the modeling.

In summary, the modeling methodology provides insights into failure mechanisms and incorporates the influence of IMC growth and surface finish diffusion barrier. The surface finish B shows longer TTF compared with A and can be characterized by a higher critical vacancy concentration threshold in the simulation.

Modeling Analysis: Design Optimization

With the abovementioned methodology, we are capable of performing analysis and predicting the EM performance of different structures. The structure with 8 vias shows no failure till 2000 h no matter whether it has surface finish A or B plating, and the simulation further validates that the TTF of structures with 8 vias can endure more than 3000 h. However, although multiple vias can help increase EM performance, implementing vias during manufacturing will increase the cost [18]. In Fig. 10, a 4-via structure is designed to reduce the cost compared with the 8-via structure. Based on the modeling results, it shows a similar failure mechanism that voids initiate

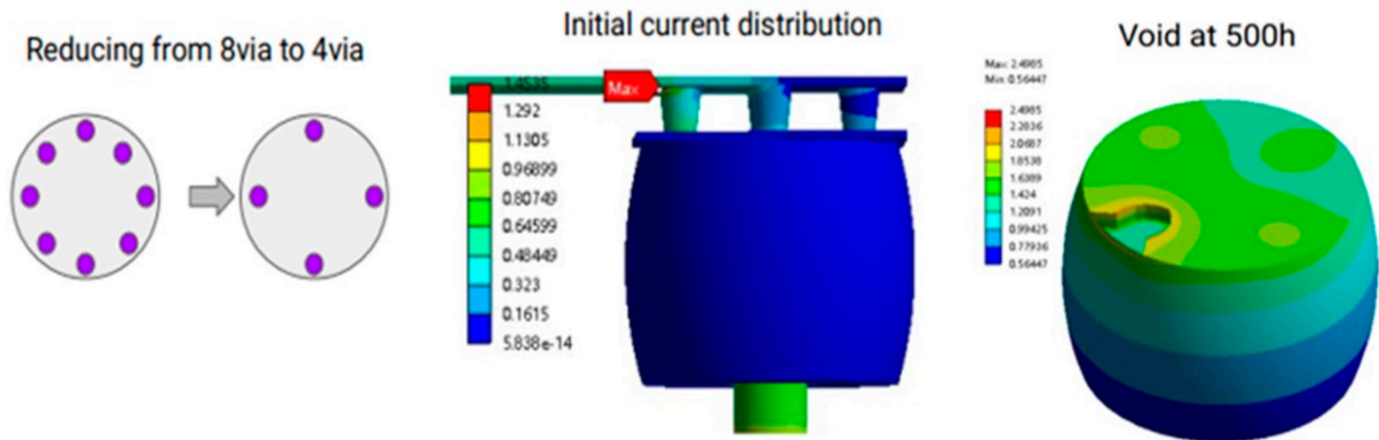

Fig. 10. Modeling results of 4-via structure.

underneath the critical via. The TTF of 4-via structure with surface A is 2400 h, which is worse than the 8-via case but still shows improvement compared with no-via case.

With the proposed FEM approach, it becomes possible to optimize the design of the structure to achieve a cost-effective balance.

Conclusions

In this study, an innovative FEM methodology is proposed to not only simulate the crack propagation behavior of the conductor under current loading, but also introduce the critical vacancy concentration threshold to characterize the diffusive influence of IMC growth and surface finish. Two different structures with surface finish A and B are compared and correlated with the modeling results. Different surface finish plating results are correlated with the testing data at 5A and 9A. With the fitted results, TTF at 7A can be predicted and validated.

Based on the simulation results, the current crowding effect could be significantly reduced by 8 vias, which is consistent with the experimental data that the structures with 8 vias show longer TTF than the ones without vias. We introduced a void nucleation threshold in FEA to reflect the impact from surface finishing as a diffusion barrier. The surface finish B has a higher void nucleation threshold due to the Nickel content. The influence of surface finish is also introduced to simulate the diffusion barrier effect because of the chemical composition difference. With the proposed model, this study further investigates the feasibility to reduce the contact window area by changing the 8 vias to 4 vias while still meeting the EM specification requirement as a cost-effective tradeoff. The study shows better EM resistance with 8 and 4 vias than no-via traces and helps predict the EM life of different structures to provide guidance for design optimization.

References

[1] J. Ha, C. Cai, P. Yin, Y. Lai, K. Pan, J. Yang, and S. Park, “Shape dependency of fatigue life in solder joints of chip resistors,” IEEE 72nd Electronic Components and Technology Conference (ECTC), pp. 1489-1494, IEEE, San Diego, US, 31 May 2022.

[2] Y. Lai, K. Pan, C. Cai, P. Yin, J. Yang, and S. Park, “Smarter temperature setup for reflow oven to minimize temperature variation among components,” *IEEE Transactions on Components, Packaging, and Manufacturing Technology*, Vol. 12, No. 3, pp. 562-569, 2022.

[3] J.R. Lloyd, “Electromigration in integrated circuit conductors,” *Journal of Physics D, Applied Physics*, Vol. 32, No. 17, p. R109, 1999.

[4] R.L. De Orio, H. Ceric, and S. Selberherr, “Physically based models of electromigration: From Black’s equation to modern TCAD models,” *Microelectronics and Reliability*, Vol. 50, No. 6, pp. 775-789, 2010.

[5] H.B. Qin, W. Yue, C.B. Ke, M.B. Zhou, X.P. Zhang, and B. Li, “Interaction effect between electromigration and microstructure evolution in BGA structure Cu/Sn-58Bi/Cu solder interconnects,” 15th International Conference on Electronic Packaging Technology, pp. 587-591, IEEE, Chengdu, China, 12 August 2014.

[6] W. Li and C.M. Tan, “Enhanced finite element modelling of Cu electromigration using ANSYS and MATLAB,” *Microelectronics Reliability*, Vol. 47, No. 9-11, pp. 1497-1501, 2007.

[7] T. Nemoto, A.T. Yokobori, Jr., and T. Murakawa, “A theoretical analysis of electromigration failure in aluminum interconnections,” *Japanese Journal of Applied Physics*, Vol. 45, No. 7R, p. 5716, 2006.

[8] L. Niu, X. Tian, and F. Jia, “The study on electromigration of solder joints under thermal cycling load,” 22nd International Conference on Electronic Packaging Technology (ICEPT), pp. 1-5, IEEE, Xiamen, China, 14 September 2021.

[9] E.E. Antonova and D.C. Looman, “Finite elements for electromigration analysis,” IEEE 67th Electronic Components and Technology Conference (ECTC), pp. 862-871, IEEE, lake buena vista, US, 30 May 2017.

[10] J. Xu, S. McCann, H. Wang, J. Wang, V. Pham, S.R. Cain, G. Refai-Ahmed, and S.B. Park, “An assessment of electromigration in 2.5 D packaging,” IEEE 69th Electronic Components and Technology Conference (ECTC), pp. 2150-2155, IEEE, Las Vegas, US, 28 May 2019.

[11] W. Tian, Y. Zhang, Y. Chen, S. Chen, and H. Cui, “Simulation research on electromigration of BGA devices,” 22nd International Conference on Electronic Packaging Technology (ICEPT), pp. 1-5, IEEE, Xiamen, China, 14 September 2021.

[12] I.A. Blech and C. Herring, “Stress generation by electromigration,” *Applied Physics Letters*, Vol. 29, No. 3, pp. 131-133, 1976.

[13] C. Cai, J. Xu, Y. Lai, J. Yang, H. Wang, S. Ramalingam, G. Refai-Ahmed, and S.B. Park, “Evaluation of electromigration coupling different physics fields in numerical simulation,” International Electronic Packaging Technical Conference and Exhibition, Vol. 86557, p. V001T05A003, American Society of Mechanical Engineers, Garden Grove, US, 25 October 2022.

[14] K. Weide-Zaage, J. Zhao, J. Ciptokusumo, and O. Aubel, “Determination of migration effects in Cu-via structures with respect to process-induced stress,” *Microelectronics and Reliability*, Vol. 48, No. 8-9, pp. 1393-1397, 2008.

[15] C.Y. Ho, J.G. Duh, C.W. Lin, C.J. Lin, Y.H. Wu, H.C. Hong, and T.H. Wang, “Microstructural variation and high-speed impact responses of

Sn–3.0 Ag–0.5 Cu/ENEPIG solder joints with ultra-thin Ni–P deposit," *Journal of Materials Science*, Vol. 48, No. 6, pp. 2724-2732, 2013.

[16] J. Xu, C. Cai, V. Pham, K. Pan, H. Wang, and S. Park, "A comprehensive study of electromigration in lead-free solder joint," IEEE 70th Electronic Components and Technology Conference (ECTC), pp. 284-289, IEEE, lake buena vista, US, 3 June 2020.

[17] J. Xu, S. McCann, H. Wang, V. Pham, S.R. Cain, G. Refai-Ahmed, and S.B. Park, "Time 0 void evolution and effect on electromigration," IEEE 69th Electronic Components and Technology Conference (ECTC), pp. 2331-2336, IEEE, May 2019.

[18] C.-H. Chien, C.-K. Lee, C.-T. Lin, Y.-M. Lin, C.-J. Zhan, H.-H. Chang, C.-K. Hsu, H.-C. Fu, W.-W. Shen, and Y.-W. Huang, "Process, assembly and electromigration characteristics of glass interposer for 3D integration," IEEE 64th Electronic Components and Technology Conference (ECTC), pp. 1891-1895, IEEE, lake buena vista, US, 27 May 2014.